PHYSICAL REVIEW D **82,** 043517 (2010)

Long-lived time-dependent remnants during cosmological symmetry breaking: From inflation to the electroweak scale

Marcelo Gleiser,[1,*] Noah Graham,[2,†] and Nikitas Stamatopoulos[1,‡]

[1]*Department of Physics and Astronomy, Dartmouth College, Hanover, New Hampshire 03755, USA*
[2]*Department of Physics, Middlebury College, Middlebury, Vermont 05753, USA*

(Received 28 April 2010; published 16 August 2010)

Through a detailed numerical investigation in three spatial dimensions, we demonstrate that long-lived time-dependent field configurations emerge dynamically during symmetry breaking in an expanding de Sitter spacetime. We investigate two situations: a single scalar field with a double-well potential and an SU(2) non-Abelian Higgs model. For the single scalar, we show that large-amplitude oscillon configurations emerge spontaneously and persist to contribute about 1.2% of the energy density of the Universe. We also show that for a range of parameters, oscillon lifetimes are *enhanced* by the expansion and that this effect is a result of parametric resonance. For the SU(2) case, we see about 4% of the final energy density in oscillons.

DOI: 10.1103/PhysRevD.82.043517 PACS numbers: 98.80.Cq, 11.10.Lm, 11.15.Ex

I. INTRODUCTION

Spontaneous symmetry breaking plays a key role in our current understanding of particle physics and is expected to have been a major factor in determining the physical properties of the early Universe [1]. In cosmology, two aspects of symmetry breaking are of great interest: it typically happens far from thermal equilibrium and it is inherently nonlinear. In the context of the electroweak phase transition, for example, an initially thermalized state is tossed out of equilibrium as the Higgs evolves to acquire a nonzero expectation value. In inflation, a nonthermal state thermalizes to reheat the Universe with an explosive energy transfer from the inflaton to other field modes. It is thus of great interest to study the dynamics of symmetry breaking in an expanding background numerically in order to isolate key features that may escape analytical techniques.

Here, we report results on three-dimensional simulations for two situations: a single, self-interacting scalar field with a double-well potential, and an SU(2) non-Abelian Higgs model. In Refs. [2,3] results have been obtained for the case of a single scalar in one dimension. It was shown that long-lived, time-dependent field configurations known as oscillons [4–6] emerged spontaneously and contributed an amazing 50% of the total energy density. These initial results triggered the present study in the context of more realistic models. There are two broad classes of scalar field oscillons that have been studied in the literature, small and large-amplitude. Small-amplitude oscillons do not probe the highly nonlinear domain of the potential, and typically have large spatial widths [3,7,8]. Their small amplitude makes it possible to study them using linearization techniques. Large-amplitude oscillons are harder to investigate analytically [9–11]. Simulations of scalar models in static two-dimensional and three-dimensional backgrounds [12] and expanding one-dimensional backgrounds [2,3] indicate that mostly large-amplitude oscillons are excited during symmetry breaking. As we show next, this is also the case for an expanding three-dimensional spacetime. The situation is different for SU(2) models, as we explain below.

This paper is organized as follows: in the next section, we introduce the scalar field model in an expanding Universe and discuss its lattice implementation. We report our results for a double-well potential, showing that oscillons contribute about 1.2% of the energy density. In Sec. III, we show that, contrary to naive expectation, for certain values of the expansion rate oscillons may have their lifetimes enhanced. We explain this result analytically by making use of parametric resonance. In Sec. IV, we introduce the SU(2) non-Abelian Higgs model and discuss its lattice implementation in an expanding Universe. In Sec. V, we discuss the results for this model. In particular, we show that, as in the case of a real scalar field, oscillons contribute a nontrivial percentage of the total energy density. Furthermore, our results indicate that the cosmological expansion seems to favor the formation of oscillons for a wider range of parameters as compared to the static case, where oscillons were found only in a 2:1 mass ratio for the Higgs and gauge boson. In Sec. VI, we briefly discuss possible application of oscillons in cosmology, which we hope to explore in forthcoming work, and conclude with a summary of our results.

*mgleiser@dartmouth.edu
†ngraham@middlebury.edu
‡nstamato@dartmouth.edu

II. SCALAR FIELD MODEL

We consider a scalar field $\Phi(\mathbf{x}, t)$ propagating in $(3+1)$-dimensional de Sitter spacetime with Hubble constant $H = \dot{a}/a$ and a double-well potential $V(\Phi) = (\lambda/4)[\Phi^2 - \mu^2/\lambda]^2$. Using $\hbar = c = k_B = 1$ and defining dimensionless variables $\phi = \Phi(\mu/\sqrt{\lambda})^{-1}$ and $\tilde{x}^\nu = \mu x^\nu$ ($\nu = 0, 1, 2, 3$), the equation of motion satisfied by ϕ is

$$\ddot{\phi} + 3\frac{\dot{a}(t)}{a(t)}\dot{\phi} = \frac{\nabla^2\phi}{a(t)^2} + \phi - \phi^3, \tag{1}$$

where overdot and ∇ denote derivatives with respect to dimensionless time $\tilde{x}^0$ and space $\tilde{x}^i$. The expansion rate becomes $H = \mu\tilde{H}$, where $\tilde{H} \equiv d\ln(a)/d\tilde{x}^0$.

Our initial conditions simulate quasithermal states of the free massive scalar field. The parameters that control the distribution of the lattice modes are the temperature T and the mass of the field $m = \mu\sqrt{2}$. The simulation space consists of a cube with comoving size L and volume $V = L^3$ discretized on a regular lattice with spacing $\Delta x^i = \Delta r$ ($i = 1, 2, 3$). We apply periodic boundary conditions and label the free field's normal modes by $\mathbf{k} = (2\pi\mathbf{n}_i/L)$, where $\mathbf{n} = (n_x, n_y, n_z)$ and the n_i are integers $n_i = -N/2 + 1 \ldots N/2$. Here $N = L/\Delta r$ is the number of lattice points per side. Each free mode is described by a harmonic oscillator with frequency $\omega_k^2 = (2\sin(k\Delta r/2)/\Delta r)^2 + m^2$, where $k = |\mathbf{k}|$. The initial conditions for the field ϕ are then given by

$$\begin{aligned}\phi(\mathbf{r}, t=0) &= \frac{1}{\sqrt{V}}\sum_{\mathbf{k}}\sqrt{\frac{\hbar}{2\omega_k}}[\alpha_k e^{i\mathbf{k}\cdot\mathbf{r}} + \alpha_k^* e^{-i\mathbf{k}\cdot\mathbf{r}}],\\ \dot{\phi}(\mathbf{r}, t=0) &= \frac{1}{\sqrt{V}}\sum_{\mathbf{k}}\sqrt{\frac{\hbar\omega_k}{2}}[\alpha_k e^{i\mathbf{k}\cdot\mathbf{r}} - \alpha_k^* e^{-i\mathbf{k}\cdot\mathbf{r}}],\end{aligned} \tag{2}$$

where α_k is a random complex variable with phase distributed uniformly on $[0, 2\pi)$ and magnitude drawn from a Gaussian distribution such that $\langle|\alpha_k|^2\rangle = [\coth(\hbar\omega_k/2T) - 1]/2$. This is the amplitude distribution for a quantum harmonic oscillator [13] with the zero-point motion subtracted. On average, modes with $\hbar\omega_k \lesssim T$ get assigned energy T, in agreement with equipartition, while the energy per mode goes rapidly to zero for $\hbar\omega_k \gtrsim T$. We thus need a lattice fine enough to resolve the high k modes that are excited at high temperatures. Using a value of Δr_0 that is at least 10 times smaller than the wavelength of the mode satisfying $\hbar\omega_k \sim T$ is enough to provide a good continuum limit.

We discretize the equation of motion using second-order space derivatives with lattice spacing Δr in all directions. We then step forward in time using a fourth-order Rünge-Kutta method. By the Courant condition, we need to keep $\Delta t < a(t)\Delta r$ at all times. We impose a maximum physical lattice spacing $\Delta r_{\max}$ that is fine enough to resolve field configurations at physical sizes that we expect for oscillons. When $a(t)\Delta r \geq \Delta r_{\max}$, we refine the lattice by bringing the lattice spacing back to $\Delta r_{\max}/2$ and inserting points by polynomial interpolation. We pick $\Delta r_{\max}$ and Δt small enough so that any further reduction does not significantly affect the final configuration of a run. All our simulations maintain energy conservation to a part in 10^3 or better.

We evolve the field $\phi(\mathbf{x}, t)$ in a box with 256^3 lattice points and $\Delta r_0 = 0.05\mu^{-1}$. We keep $\Delta t = 0.01\mu^{-1}$ constant throughout the simulation. As the lattice spacing increases to $\Delta r_{\max} = 0.5\mu^{-1}$, we insert points in the lattice, bringing the spacing down to $\Delta r_{\max}/2$. We vary the values of the expansion factor H and the initial temperature T and evolve the field until it cools down to $T/a(t) = 0.3\mu$. After the Universe has expanded and cooled, we observed persistent localized structures as peaks in the energy density. We show a typical sequence of snapshots in Fig. 1.

By isolating these peaks individually, we find that they all share the typical signatures of spherically symmetric oscillon configurations: their centers oscillate with the typical oscillon frequency, as shown in the inset of Fig. 2, and their energies coincide with the plateau energies found in detailed oscillon studies [5,6,10]. The energy of a configuration is calculated by integrating the field's total energy around its peak using a radius $r = 10\mu^{-1}$. We consistently found $E_{\rm osc} \simeq 45\mu/\lambda$. We then measured the fraction of energy in oscillons (Fig. 2) and the number of oscillons nucleated as a function of temperature, which scales simply as $N_{\rm osc} \propto V = L^3 \propto T^3$.

Although we quote results for $H = 0.01\mu$, we have performed simulations for a slower expansion rate of $H = 0.005\mu$ obtaining similar qualitative behavior: for a wide range of initial temperatures, $\rho_{\rm osc}/\rho_{\rm tot} = \Omega_{\rm osc} \sim 1.2\%$. Smaller values of H require impractical computation time, but we do not expect any qualitative changes. We note that since the simulations end with fairly large values of $\Delta r = 0.5\mu^{-1}$, our results are lower bounds on $\rho_{\rm osc}$. Of course, scalar field oscillons are not stable in three dimensions and will decay after $\tau_{\rm osc} \sim 10^4\mu^{-1}$. Nevertheless, during their lifetime, they may be responsible for several important effects, as we discuss in section VI. We also note that oscillons are prevented from forming if the horizon size $1/H$ is of the order of the oscillon size, $R_{\rm osc} \sim 4\mu^{-1}$. For $H \gtrsim 0.1\mu$, which fortunately is not very realistic, large-amplitude fluctuations are flattened out before the stabilizing effect of nonlinearities can kick in. In other words, for oscillons to be cosmologically viable, we must have $R_{\rm osc}/\lambda_H = \tilde{R}_{\rm osc}\tilde{H} \ll 1$, where $\lambda_H = H^{-1}$ is the horizon length. This condition is easily satisfied for physics below the Planck scale.

III. LIFETIME ENHANCEMENT

Having established that oscillons emerge dynamically in an expanding background, we need to examine how the

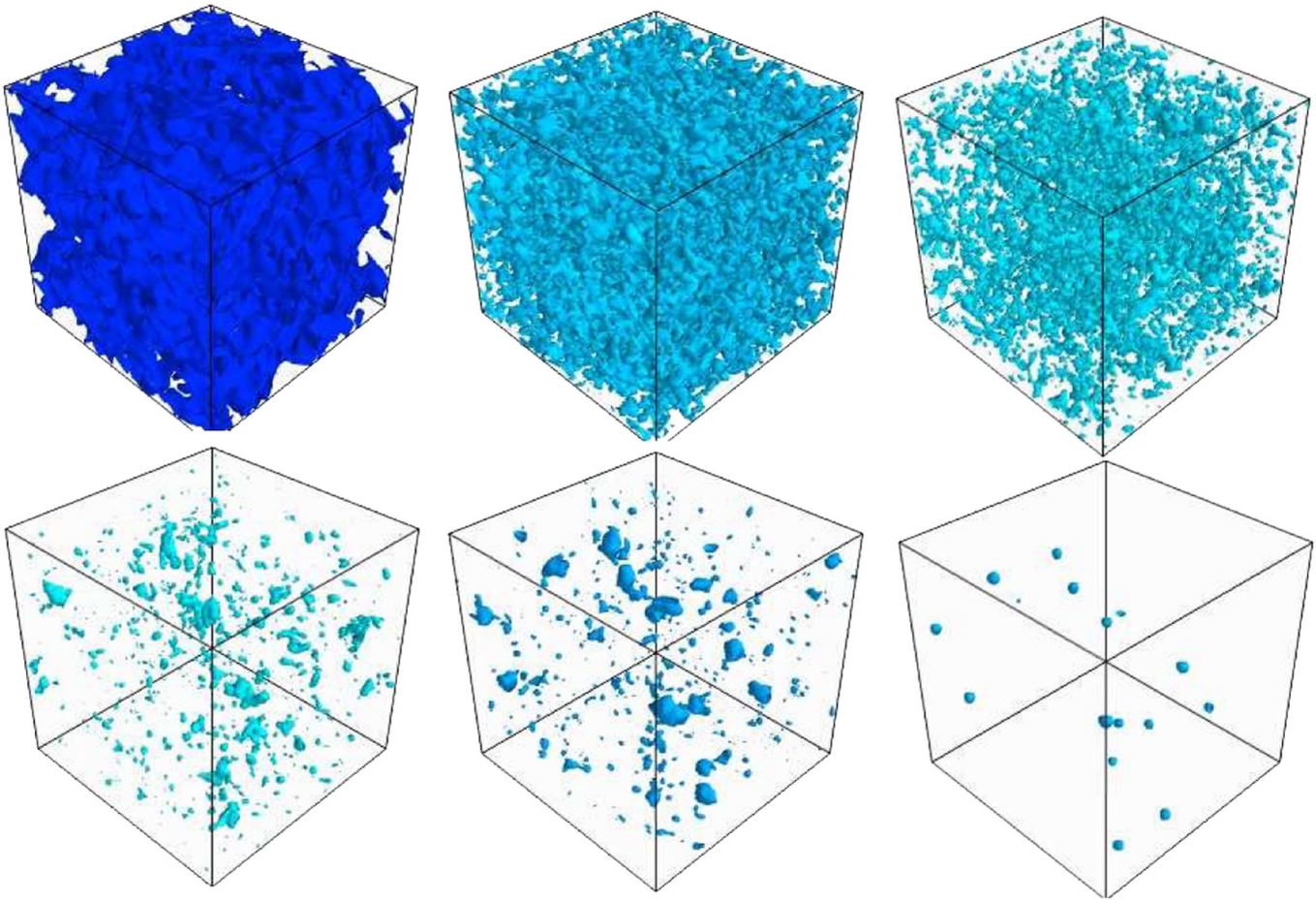

FIG. 1 (color online). Sequence of time snapshots of the energy density. Time increases from left to right and top to bottom at times $t\mu = 0, 50, 100, 150, 200, 250$, $H = 0.01\mu$, and $T = 6.0\mu$. All snapshots show the energy density u with an isosurface at $u = 0.2\mu^4$.

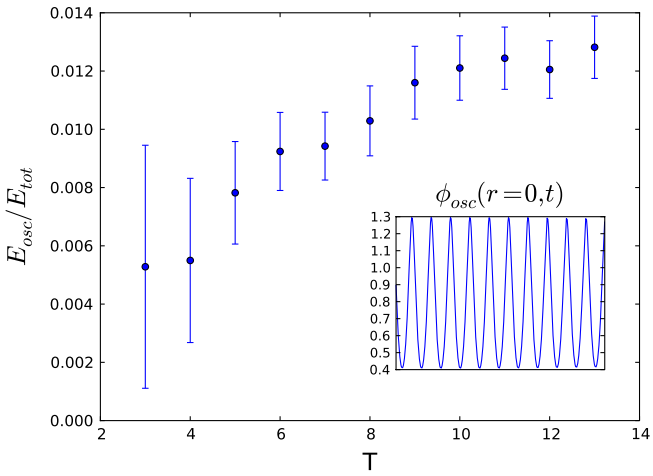

FIG. 2 (color online). Fraction of energy in oscillons as a function of temperature in units of μ. Here $\Delta r_0 = 0.05\mu^{-1}$, $\Delta r_{\max} = 0.5\mu^{-1}$, and $H = 0.01\mu$. Error bars denote ensemble averages over 10 runs. The inset shows the near-harmonic oscillations of the oscillon core. A simulation of a typical run can be viewed at [14]

expansion affects their lifetime. For numerical efficiency, we exploit the spherical symmetry of the final oscillon configuration and reduce our system to an effectively one-dimensional problem by letting $\nabla^2\phi \to \partial^2\phi/\partial r^2 + (2/r)\partial\phi/\partial r$ in Eq. (1). We find oscillons by setting the initial field configuration to be Gaussian, $\phi(r, 0) = 2\exp(-r^2/R_0^2) - 1$, with boundary conditions $\phi(r \to \infty, t) = -1$, $\phi'(0, t) = 0$, and $\dot{\phi}(r, 0) = 0$ [5,6]. In the absence of expansion, Gaussians with $2.4 \lesssim R_0\mu \lesssim 4.5$ settle into long-lived oscillon configurations.

We follow the same procedure as in three dimensions so that as soon as the lattice spacing becomes $\Delta r_{\max} = 0.1\mu^{-1}$, $L_{\max} \gtrsim 2/H$, we insert points via polynomial interpolation, and bring the lattice spacing back to $\Delta r = 0.05\mu^{-1}$. We then truncate the box to $L \gtrsim 1/H$, which cannot affect the oscillon at $r = 0$. We always use a box of initial size $L_0 = 1/H + 50\mu^{-1}$ in natural units, and we have verified that any run with $L_0 \gtrsim 1/H$ gives identical results. In Fig. 3, we show the effects of expansion for a sample of initial configurations. There is a clear symmetry about $R_0 = 2.86\mu^{-1}$, the longest-lived oscillon in the

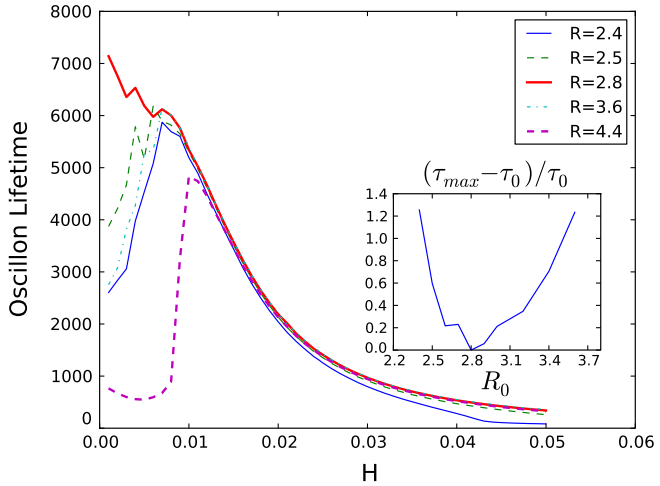

FIG. 3 (color online). Lifetime, in units of μ^{-1}, for oscillons formed from Gaussians with $2.4 \leq R\mu \leq 4.4$, as a function of expansion rate H in units of μ. The inset shows the maximal fractional increase in oscillon lifetime for different radii at $H_{\max}$.

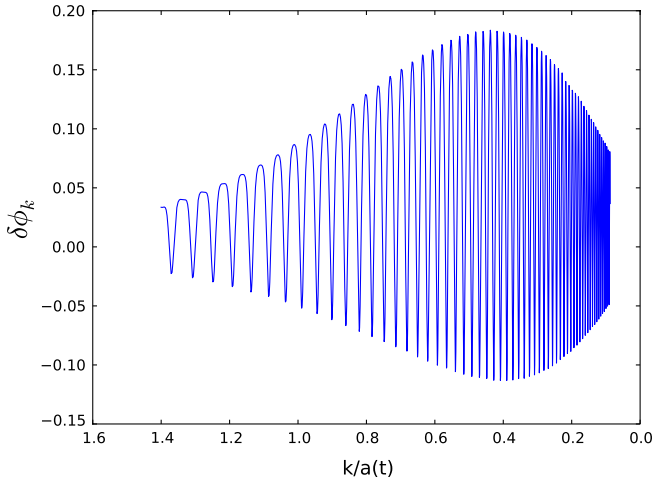

FIG. 4 (color online). Oscillations in $\delta\phi(k, t)$ for an oscillon with $R_0 = 2.5\mu^{-1}$ and expansion rate $H = 0.006\mu$, at times $3200 \leq t\mu \leq 3700$. Here we plot a mode which starts at $k/a \simeq 1.4\mu$ and gets redshifted to $k/a \simeq 0.1\mu$. As k/a gets smaller, the mode enters the resonance window, and its Fourier component gets amplified and then redshifted away. In this case, $\omega \simeq 1.4\mu$ ($< m = \sqrt{2}\mu$) and $C = 1.8\mu^2$, with $A_k = 4$ for $k/a \simeq 0.4\mu$, which is the dominant wave vector of this oscillon ($R \simeq 2.9\mu^{-1}$).

absence of expansion: radii to both sides of $R_0 = 2.86\mu^{-1}$ experience an increase in lifetime for a range of H, with the increase being more pronounced for shorter lifetimes. The longest-lived oscillon, in turn, does not experience any noticeable enhancement. The inset of Fig. 3 shows the maximum fractional increase in lifetime $(\tau_{\max} - \tau_0)/\tau_0$ as a function of initial radius R_0. The lifetime enhancement follows an approximate scaling law around $R_0 = 2.86\mu^{-1}$, $\tau_{\rm osc}\mu \sim |R_0\mu - 2.86|^{0.05}$.

To understand the origin of the lifetime enhancement caused by the expansion, we decompose the field as $\phi(\mathbf{x}, t) = \phi_{av}(t) + \delta\phi(\mathbf{x}, t)$, where ϕ_{av} is the volume averaged field. Linearizing Eq. (1) with respect to $\delta\phi(\mathbf{x}, t)$ and taking the Fourier transform, we obtain (for $k > 0$)

$$\delta\ddot{\phi}(k, t) + 3H\delta\dot{\phi}(k, t) + \left(\frac{k^2}{a(t)^2} + V''(\phi_{av}(t))\right)\delta\phi(k, t) = 0. \tag{3}$$

Once the Gaussian has settled into the oscillon stage, $V''(\phi_{av}(t))$ can be approximated by $V''(\phi_{av}(t)) = \Phi_0\cos(\omega t) + C$, where Φ_0 and C vary very slowly during an oscillon's lifetime and depend on the value of the initial radius R_0 and the Hubble constant H. Here $\omega < m$ is the oscillon's frequency of oscillation. Introducing new variables $\omega t = 2z - \pi$, and $\delta\phi = \exp(-3Hz/\omega)\chi$, Eq. (3) becomes

$$\chi'' + [A_k - 2q\cos 2z]\chi = 0, \tag{4}$$

where $A_k = \frac{1}{\omega^2}[4k^2/a^2 + 4C - 9H^2]$, $q = 2\Phi_0/\omega^2$, and prime denotes differentiation with respect to the new variable z. Equation (4) is the Mathieu equation, which is known to exhibit parametric resonance when $A_k \simeq l^2$, $l = 1, 2, \ldots$ [15]. Thus, particular combinations of values of C, H and ω can lead to exponential amplification in the oscillations of χ, and consequently $\delta\phi(k, t)$, at certain modes k/a. Because C is a positive number, the $A_k \simeq 1$ resonance window occurs for real values of k/a only for very large values of H, which destabilize the oscillon before it can lead to resonance. The $A_k \simeq 9$ and higher windows lead to resonances that are too weak to overcome the damping due to the expansion. The $A_k \simeq 4$ window, however, can lead to parametric amplification of the dominant oscillon wave vectors for the values of H that generate the observed lifetime enhancement depicted in Fig. 3.

The $A_k \simeq 4$ resonance window leads to exponential amplification to the oscillations in $\chi \propto e^{\xi z}$, where $\xi \simeq \sqrt{5}q^2/48$ [16]. For small values of H, the amplification overcomes the damping due to expansion. For higher values of H, the damping overcomes the amplification, and the oscillon decays. An example is shown in Fig. 4.

IV. SU(2) MODEL: IMPLEMENTATION

Because the SU(2) model is considerably more expensive numerically to simulate, the range of experiments we can carry out is limited. However, these experiments show very similar behavior to the scalar model. We begin from the Lagrangian density in the absence of expansion,

$$\mathcal{L} = -\tfrac{1}{4}\boldsymbol{F}_{\mu\nu}\cdot\boldsymbol{F}^{\mu\nu} + (D_\mu\Phi)^\dagger(D^\mu\Phi) - \lambda(|\Phi|^2 - \mu^2)^2, \tag{5}$$

where the boldface vector notation refers to isovectors. Here the Higgs field Φ is an SU(2) doublet, and the SU(2) field strength and covariant derivatives are

$$\boldsymbol{F}_{\mu\nu} = \partial_\mu \boldsymbol{W}_\nu - \partial_\nu \boldsymbol{W}_\mu - g\boldsymbol{W}_\mu \times \boldsymbol{W}_\nu, \tag{6}$$

$$D_\mu \Phi = \left(\partial_\mu + i\frac{g}{2}\boldsymbol{\tau}\cdot\boldsymbol{W}_\mu\right)\Phi, \tag{7}$$

$$D^\mu \boldsymbol{F}_{\mu\nu} = \partial^\mu \boldsymbol{F}_{\mu\nu} - g\boldsymbol{W}^\mu \times \boldsymbol{F}_{\mu\nu}, \tag{8}$$

where $\boldsymbol{\tau}$ represents the weak isospin Pauli matrices. We obtain the equations of motion

$$D_\mu \boldsymbol{F}^{\mu\nu} = \boldsymbol{J}^\nu, \qquad D^\mu D_\mu \Phi = 2\lambda(\mu^2 - |\Phi|^2)\Phi, \tag{9}$$

where the gauge current is $\boldsymbol{J}_\nu = g\,\mathrm{Im}(D_\nu\Phi)^\dagger\boldsymbol{\tau}\Phi$ and we work in the gauge $\boldsymbol{W}_0 = \boldsymbol{0}$. With this choice, the covariant time derivatives become ordinary derivatives and we can apply a Hamiltonian formalism. The $\boldsymbol{W}_j$ fields have mass $m_W = g\mu/\sqrt{2}$, and the Higgs field has mass $m_H = 2\mu\sqrt{\lambda}$.

To include the effects of expansion, we again work in comoving coordinates with a scale factor $a(t)$. We now have the action

$$S = \int d^3\boldsymbol{r}a(t)^3\Bigg[\frac{1}{2}\sum_{j=x,y,z}(\boldsymbol{E}_j\cdot\boldsymbol{E}_j - \boldsymbol{B}_j\cdot\boldsymbol{B}_j) + \dot\Phi^\dagger\dot\Phi - \frac{1}{a(t)^2}\sum_{j=x,y,z}(\partial_j\Phi^\dagger)(\partial_j\Phi) - \lambda(|\Phi|^2-\mu^2)^2\Bigg], \tag{10}$$

where

$$\boldsymbol{E}_j = \dot{\boldsymbol{W}}_j \quad \text{and}$$
$$\boldsymbol{B}_j = -\frac{1}{2}\sum_{j',j''=x,y,z}\epsilon_{jj'j''}\left(\frac{1}{a(t)}\partial_{j'}\boldsymbol{W}_{j''} - g\boldsymbol{W}_{j'}\boldsymbol{W}_{j''}\right). \tag{11}$$

Here the dot indicates time derivative and Latin indices run over space dimensions.

For numerical computation we put the theory on a lattice, following the conventions and techniques used in [17]. The field variables are the values of the Φ^p field at the lattice sites p and the spacelike Wilson lines

$$U_j^p(t) = e^{ig\boldsymbol{W}_j^p(t)\cdot\boldsymbol{\tau}a(t)\Delta x/2}, \tag{12}$$

emanating from lattice site p in the spacelike direction j. Since the lattice equations are second order, we will find each field at the next time slice based on the previous two. We let t be the time for the current set of lattice points and spacelike links and define $t_+ = t + \Delta t$ and $t_- = t - \Delta t$ to be the subsequent and previous times, respectively. We also take $t_{+/2} = t + \Delta t/2$ and $t_{-/2} = t - \Delta t/2$ to be the times in between, which will be the times at which we evaluate the timelike links.

We define the Wilson line for the link emanating from lattice site p in the negative jth direction to be the adjoint of the corresponding Wilson line emanating in the positive direction from the neighboring site, $U_{-j}^p(t) = U_j^{p-j}(t)^\dagger$, where the notation $p \pm j$ indicates the adjacent lattice site to p, displaced from p in direction $\pm j$. At the edges of the lattice we use periodic boundary conditions. We define the elements of the field strength tensor, which are centered on the timelike and spacelike plaquettes of the lattice,

$$\boldsymbol{\tau}\cdot\boldsymbol{E}_j^p(t_{+/2}) = \frac{2}{iga(t_{+/2})\Delta x\Delta t}\log U_j^p(t_+)U_j^p(t)^\dagger \quad \text{and}$$
$$\boldsymbol{\tau}\cdot\boldsymbol{B}_j^p(t) = \frac{i}{g(a(t)\Delta x)^2}\sum_{j',j''=x,y,z}\epsilon_{jj'j''}U^p_{\square(j',j'')}(t), \tag{13}$$

where $U^p_{\square(j,j')}(t) = U_j^p(t)U_{j'}^{p+j}(t)U_{-j}^{p+j+j'}(t)U_{-j'}^{p+j'}(t)$, and we have defined the logarithm of a 2×2 matrix in the form of Eq. (12) as

$$\log U_j^p(t) = \frac{iga(t)\Delta x}{2}\boldsymbol{W}_j^p(t)\cdot\boldsymbol{\tau}. \tag{14}$$

We note that $\log XY \neq \log X + \log Y$ when the matrices do not commute. The logarithms and exponentials needed to convert between the group and the algebra can be computed efficiently using

$$e^{i\theta\hat{\boldsymbol{n}}\cdot\vec{\boldsymbol{\tau}}} = \cos\theta + i\hat{\boldsymbol{n}}\cdot\vec{\boldsymbol{\tau}}\sin\theta = \begin{pmatrix}\cos\theta + i\hat{\boldsymbol{n}}_z\sin\theta & i\hat{\boldsymbol{n}}_x\sin\theta + \hat{\boldsymbol{n}}_y\sin\theta \\ i\hat{\boldsymbol{n}}_x\sin\theta - \hat{\boldsymbol{n}}_y\sin\theta & \cos\theta - i\hat{\boldsymbol{n}}_z\sin\theta\end{pmatrix}, \tag{15}$$

where $\hat{\boldsymbol{n}}$ is a unit vector and the link matrices have $\hat{\boldsymbol{n}}\theta = \boldsymbol{W}_j^p(t)ga(t)\Delta x/2$. For efficiency, we replace $\sin\theta \to \theta$ and $\cos\theta \to \sqrt{1-\theta^2}$ when computing both the logarithm and the corresponding exponential. This discretization then is equivalent (without expansion) to what is used in other numerical studies of electroweak symmetry-breaking dynamics [18–21].

We find the equation of motion for the Higgs field

$$\Phi^p(t_+) = \frac{1}{1+\frac{3H\Delta t}{2}}\Bigg[2\Phi^p(t) - \left(1 - \frac{3H\Delta t}{2}\right)\Phi^p(t_-) + \Delta t^2\ddot\Phi^p(t)\Bigg], \tag{16}$$

where $H = \frac{\dot a(t)}{a(t)}$ is the Hubble constant and

$$\ddot\Phi^p(t) = \sum_{j=\pm x,\pm y,\pm z}\frac{U_j^p(t)\Phi^{p+j}(t) - \Phi^p(t)}{a(t)^2\Delta x^2} + 2\lambda(\mu^2 - |\Phi^p(t)|^2)\Phi^p(t). \tag{17}$$

For the gauge fields, we have

$$U_j^p(t_+) = \Bigg(\exp\Bigg\{\log(U_j^p(t)U_j^p(t_-)^{H\Delta t/2-1}) - \Bigg[\sum_{j'\neq j}\Bigg(\frac{\log U^p_{\Box(j,j')}(t) + \log U^p_{\Box(j,-j')}(t)}{a(t)^2\Delta x^2}\Bigg) + \frac{ia(t)\Delta x}{2} g\boldsymbol{J}_j^p(t)\cdot\boldsymbol{\tau}\Bigg]\Delta t^2\Bigg\}U_j^p(t)\Bigg)^{1/(H\Delta t/2+1)}, \tag{18}$$

where the gauge current is

$$\boldsymbol{J}_j^p(t) = g\,\mathrm{Im}\frac{\Phi^p(t)^\dagger\boldsymbol{\tau}U_j^p(t)\Phi^{p+j}(t)}{a(t)\Delta x}, \tag{19}$$

and the logarithm in Eq. (14) is used to compute the exponents in Eq. (18).

Assuming it is obeyed by the initial conditions, time evolution preserves the Gauss's law constraint,

$$\sum_{j=x,y,z}\frac{\boldsymbol{E}_j^p(t_{+/2}) + \boldsymbol{E}_{-j}^p(t_{+/2})}{a(t_{+/2})\Delta x} = \boldsymbol{J}_0^p(t_{+/2}), \tag{20}$$

where the charge density is given by

$$\boldsymbol{J}_0(t_{+/2}) = g\,\mathrm{Im}\Bigg(\frac{\Phi^p(t_+) - \Phi^p(t)}{\Delta t}\Bigg)^\dagger\boldsymbol{\tau}\Phi^p(t). \tag{21}$$

Energy is not conserved because in the expanding background we have $dU = -pdV$, where p is the pressure. In the lattice model we then have

$$\frac{dU}{dt} = -(a(t)\Delta x)^3 H\sum_p\Bigg[\frac{1}{2}\sum_{j=x,y,z}(\boldsymbol{E}_j^p\cdot\boldsymbol{E}_j^p + \boldsymbol{B}_j^p\cdot\boldsymbol{B}_j^p) + 3|\dot\Phi|^2 - \sum_{j=x,y,z}\Bigg|\frac{U_j^p\Phi^{p+j} - \Phi^p}{a(t)\Delta x}\Bigg|^2 - 3\lambda(|\Phi^p|^2 - \mu^2)^2\Bigg]. \tag{22}$$

We have verified that both the Gauss's law and energy constraints are well obeyed throughout our simulation.

We set initial conditions for the first two time-slices, which we denote as t_0 and t_1, by occupying the modes of all the components of the Higgs and gauge fields at temperature T, as in the case of a single scalar field. Then we modify these initial conditions to make them obey Gauss's law, by the following steps:

(i) First, since we have periodic boundary conditions, the total charge should be zero. To enforce this constraint, we shift the Φ^p field on both of the first two time slices t_0 and t_1 by the same constant,

$$\Phi^p \to \Phi^p - \frac{i}{g|\dot{\bar\Phi}|^2}(\bar{\boldsymbol{J}}_0\cdot\boldsymbol{\tau})\dot{\bar\Phi}, \tag{23}$$

where $\bar{\boldsymbol{J}}_0$ and $\dot{\bar\Phi}$ are the average values of $\boldsymbol{J}_0$ and $\dot\Phi$ over the lattice at time $t_{1/2}$, respectively.

(ii) Next, we fix the longitudinal component of the gauge fields, as described in Ref. [19]. We take a discrete Fourier transform of the initial charge $\boldsymbol{J}_0^p(t_{1/2})$ and gauge field $\boldsymbol{J}_j^p(t_{1/2})$ to obtain $\tilde{\boldsymbol{J}}_0^{\vec k}(t_{1/2})$ and $\tilde{\boldsymbol{W}}_j^{\vec k}(t_{1/2})$ for the initial time step, where $\vec k$ labels the Fourier transformed lattice. We then modify the initial time derivative of $\boldsymbol{W}_j^p$ (by changing its value on one of the first time slices but not the other) by sending

$$\dot{\tilde{\boldsymbol{W}}}_j^{\vec k}(t_{1/2}) \to \dot{\tilde{\boldsymbol{W}}}_j^{\vec k}(t_{1/2}) - \Bigg(\sum_{j'=x,y,z}\vec k_{j'}\dot{\tilde{\boldsymbol{W}}}_{j'}^{\vec k}(t_{1/2}) + i\tilde{\boldsymbol{J}}_0^{\vec k}(t_{1/2})\Bigg)\frac{\vec k_j}{|\vec k|^2} \tag{24}$$

and then inverting the discrete Fourier transform to obtain the modified gauge fields, which in turn give the modified Wilson loops. Note that we do not make any modification for $\vec k = \vec 0$, where this transformation breaks down; that case was already handled by the previous step.

(iii) Finally, while in an Abelian theory the subtraction of the longitudinal component would be sufficient to implement Gauss's law, for a non-Abelian theory the nonlinear term in the field strength makes this agreement only approximate. As a result, we adjust the phase of $\Phi^p(t_1)$,

$$\Phi^p(t_1) \to \frac{|\Phi^p(t_1)|}{|\Phi^p(t_0)|}\mathcal{U}^p(t_{1/2})\Phi^p(t_0) \quad\text{with}\quad \mathcal{U}^p(t_{1/2}) = \exp\Bigg[-\sum_{j=x,y,z}\frac{\log U_j^p(t_1)U_j^p(t_0)^\dagger + \log U_{-j}^p(t_1)U_{-j}^p(t_0)^\dagger}{g^2(a(t_{1/2})\Delta x)^2|\Phi^p(t_1)||\Phi^p(t_0)|/2}\Bigg], \tag{25}$$

leaving $\Phi_0^p(t_0)$ unchanged, in order to assure that Gauss's law is satisfied.

V. SU(2) MODEL: RESULTS

We begin with a universe of size $La(t=0) = 4/\mu$, temperature $T = 4\mu$, lattice spacing $a(t=0)\Delta x = 1/(224\mu)$, and use a time step $\Delta t = 1/(448\mu)$. We allow the universe to expand at a constant rate, with Hubble constant $H = \mu(\log 2)/12 \approx 0.06\mu$, and expand the universe by a factor of 224, so that the final lattice spacing is $a(t_{\mathrm{final}})\Delta x = 1/\mu$. We measure the fraction of energy in oscillons by including those points whose energy density is 4 times the average energy density. Under ordinary thermal expansion this fraction would stay constant, and during the initial stages of the expansion it is identically zero. At the

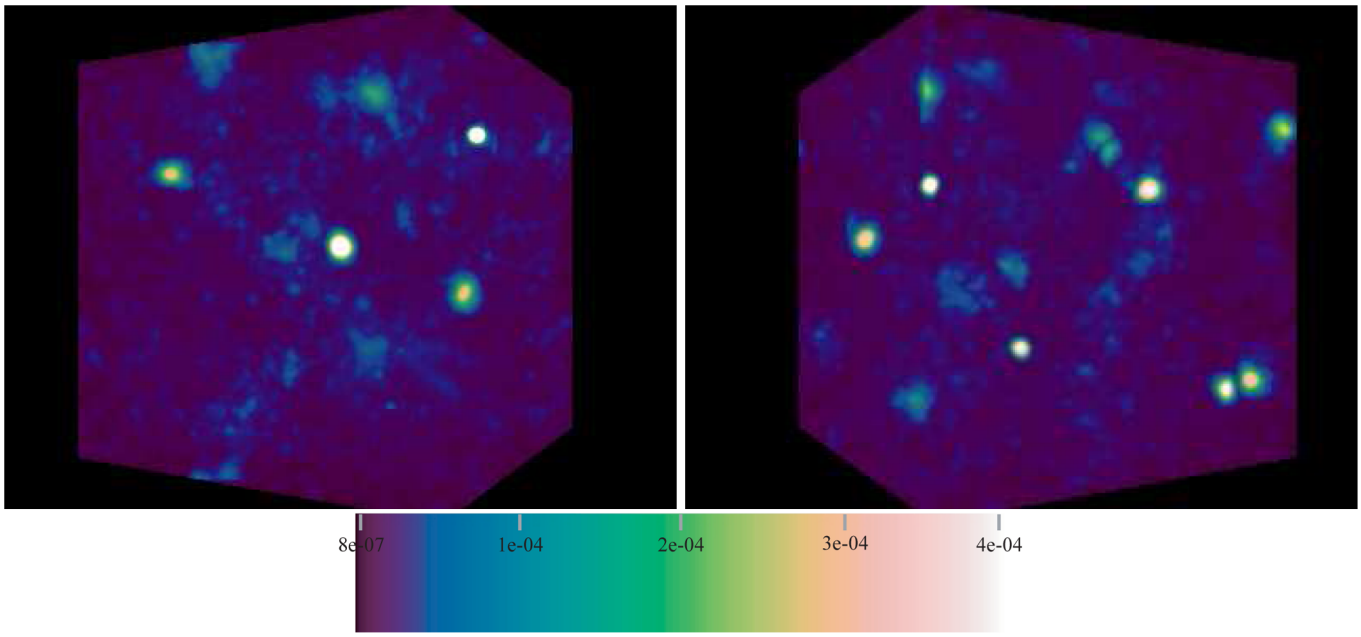

FIG. 5 (color online). Energy density in units of μ^4 at the end of the expansion for $g = \sqrt{2}$ with $\lambda = 1.0$ (left panel) and $\lambda = 1.1$ (right panel). To implement the standard model coupling of $g_{\mathrm{SM}} = 0.624$ with the same mass ratio, this energy would be scaled up by a factor of $(g/g_{\mathrm{SM}})^2$.

end of the expansion, approximately 4% of the energy is found in oscillons by this measure. The energy density is shown in Fig. 5, and the evolution of the energy over time is shown in Fig. 6. Compared to the scalar model, oscillons in the SU(2) model have smaller amplitude and larger spatial extent, requiring a larger simulation volume. The simulation is thus considerably more expensive numerically, especially given the cost of evolving a total of 13 real degrees of freedom per lattice site instead of one.

We note that similar results are seen both for $g = \sqrt{2}$, $\lambda = 1$, in which the Higgs and gauge fields are in the 2:1 mass ratio found in [17,22], and for $g = \sqrt{2}$, $\lambda = 1.1$, where the masses are not in this ratio. Because of the high numerical costs associated with the expanding background simulation, we are not able to track the stability of oscillons formed in this way over long time scales, but these results suggest that the expansion may broaden the range of parameters for which oscillons are stable. Also, by allowing oscillons to form from a thermal background rather than a fixed ansatz, this simulation is capable of scanning a wider range of configuration space (and our results clearly show that oscillon configurations represent attractors in this space). Work is currently underway to investigate these questions in greater detail.

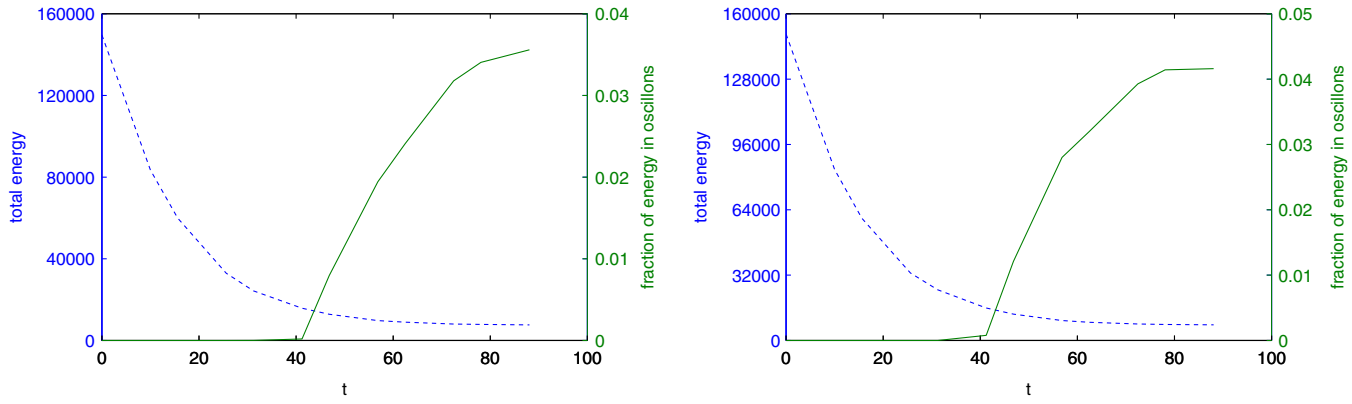

FIG. 6 (color online). Fraction of energy in oscillons (solid line) and total energy (dashed line) as a function of time. Energy is given in units of μ and time in units of $1/\mu$, with $g = \sqrt{2}$ and $\lambda = 1.0$ (left panel) and $\lambda = 1.1$ (right panel). To implement the standard model coupling of $g_{\mathrm{SM}} = 0.624$ with the same mass ratio, this energy would be scaled up by a factor of $(g/g_{\mathrm{SM}})^2$.

VI. POSSIBLE IMPACT ON COSMOLOGY AND SUMMARY

Our results indicate that oscillonlike configurations emerge dynamically during spontaneous symmetry breaking in expanding cosmological backgrounds. Furthermore, they contribute a significant fraction of the total energy density. They are thus poised to play an essential role in the dynamics of the early Universe, be it during post-inflationary reheating or during symmetry-breaking phase transitions.

In order to briefly address the impact oscillons may have on cosmology, it is best to consider different energy scales separately. For the sake of illustration, we focus on the grand unified theory (GUT) and electroweak scales, which differ by roughly 13 orders of magnitude. Also, it is important to differentiate between real scalars and Abelian and non-Abelian Higgs models. Thus, before we start, it may be useful to summarize what is known of oscillon lifetimes in these models.

As we mentioned before, for real scalar fields in three dimensions, the oscillon lifetime–with or without the enhancement from the expansion reported here–is typically $\tau_{\rm osc} \sim 10^{3-4}\mu^{-1}$ [5,10]. For models with gauge fields, the evidence at hand points to *very* large lifetimes. Studies for Abelian-Higgs models in two dimensions have not seen oscillons decaying, and report lifetimes in excess of $10^5\mu^{-1}$ [23]. Studies of Abelian-Higgs models in three dimensions obtained similar results: oscillons have been observed to persist for times $t \gtrsim 7 \times 10^5\mu^{-1}$ without decaying [24]. For non-Abelian Higgs models, the situation is similar: the data at hand indicates that once formed, oscillons live for extremely long times. Those in the gauged-SU(2) Higgs model have not been observed to decay after $t \gtrsim 5 \times 10^5\mu^{-1}$ [17,22]. Thus, although a more detailed study of Abelian and non-Abelian Higgs oscillons and their stability is clearly warranted, results so far indicate that they may be extremely long-lived, even perturbatively stable. Of course, the key question is whether their lifetime can be longer than the cosmological time scale at their formation. If that's the case, they behave as stable, localized defects.

At the GUT scale, it is clear that the oscillon lifetime is at least of order of the cosmological time scale, $\tilde{H}^{-1} \sim (M_{\rm Planck}/\mu) \sim 10^{3-4}$. Thus, for all practical purposes at GUT scales oscillons behave as stable localized defects. As has been shown elsewhere, in the context of first-order phase transitions, long-lived bubblelike configurations such as oscillons can either become a critical bubble or coalesce to become one. In both cases, the decay of the false vacuum is greatly accelerated, changing from exponentially suppressed to power-law [25]. It has been suggested that oscillons may accelerate the decay of the false vacuum during inflation, potentially solving the bubble coalescence problem of old inflation. This has been recently illustrated within the context of a modified hybrid inflation model [26].

Oscillons may also have a key impact during post-inflationary reheating. As coherent field configurations, they naturally delay the approach to equilibrium, acting as bottlenecks for equipartition [27]. As such, they may influence (decrease) the reheating temperature, a possibility we are currently investigating. An interesting open question is how these nonequilibrium results apply in the context of gauge models.

Moving on to the electroweak scale, since $\tilde{H}_{\rm ew} \sim 10^{-16}$, we are on a realm which is very distant from our numerical range of $\tilde{H} \sim 10^{-2}$. Still, we suggest that there are at least two ways in which oscillons may play a role at these relatively low energy scales. Both depend on their lifetime. If non-Abelian oscillons live for $t \sim 10^{16}\mu^{-1}$, that is, if they are perturbatively stable, they will remain active at cosmologically relevant time scales. As at the GUT scale discussed above, they may speed up vacuum decay in the context of a first-order transition (which is ruled out in the Standard Model but not in all of its extensions) or they may delay thermalization. If they persist for even longer, they may even be relevant to dark matter or baryogenesis.

On the hand, if they live for shorter times $10^4 < t\mu < 10^{16}$, their presence may still affect the dynamics of symmetry breaking. As is well-known, most phase transitions are initiated due to the presence of inhomogeneities or ''seeds'' [13]. If oscillons are present in sufficient quantities, they will modify the effective potential nonperturbatively, affecting the dynamics of the transition [28]. Although much work remains to be done to investigate such nonperturbative effects in more detail, these mechanisms suggest that even relatively short-lived oscillons will have important effects during cosmological symmetry breaking.

ACKNOWLEDGMENTS

M. G. and N. S. were partially supported by the National Science Foundation (NSF) under Grant No. PHY-0653341. N. G. was supported in part by the National Science Foundation under Grant No. PHY-0855426 and a Baccalaureate College Development grant from Vermont EPSCoR. Numerical simulations were carried out using TeraGrid resources at the National Center for Supercomputing Applications (NCSA), with support from NSF, and at the Vermont Advanced Computing Center. Visualizations were created by D. Bock (NCSA).

Note added in proof.—Recent work by M. A. Amin offers further support to our hypothesis that oscillons will have important effects in an expanding Universe [29]. We thank the author for sending his manuscript to us.

[1] A. Vilenkin and E. P. S. Shellard, *Cosmic Strings and Other Topological Defects* (Cambridge University Press, Cambridge, 1994).
[2] N. Graham and N. Stamatopoulos, Phys. Lett. B **639**, 541 (2006).
[3] E. Farhi *et al.*, Phys. Rev. D **77**, 085019 (2008).
[4] I. L. Bogolubsky and V. G. Makhankov, Pis'ma Zh. Eksp. Teor. Fiz. **24**, 15 (1976).[JETP Lett. **24**, 12 (1976)].
[5] M. Gleiser, Phys. Rev. D **49**, 2978 (1994).
[6] E. J. Copeland, M. Gleiser, and H.-R. Müller, Phys. Rev. D **52**, 1920 (1995).
[7] G. Fodor, P. Forgács, P. Grandclément, and I. Rácz, Phys. Rev. D **74**, 124003 (2006).
[8] M. A. Amin and D. Shirokoff, Phys. Rev. D **81**, 085045 (2010).
[9] M. Gleiser, Phys. Lett. B **600**, 126 (2004).
[10] M. Gleiser and D. Sicilia, Phys. Rev. Lett. **101**, 011602 (2008); Phys. Rev. D **80**, 125037 (2009).
[11] M. P. Hertzberg, arXiv:1003.3459.
[12] M. Gleiser, B. Rogers, and J. Thorarinson, Phys. Rev. D **77**, 023513 (2008); M. Gleiser and R. Howell, Phys. Rev. Lett. **94**, 151601 (2005).
[13] L. D. Landau and E. M. Lifshitz, *Statistical Physics Part 1* (Pergamon Press, Oxford, 1980), 3rd ed..
[14] http://www.youtube.com/watch?v=_0co05XkNMY (Web link on electronic version)
[15] L. Kofman, A. Linde, and A. Starobinsky, Phys. Rev. D **56**, 3258 (1997).
[16] N. W. Mac Lachlan, *Theory and Application of Mathieu functions* (Dover, New York, 1961).
[17] N. Graham, Phys. Rev. Lett. **98**, 101801 (2007); **98**, 189904(E) (2007); Phys. Rev. D **76**, 085017 (2007).
[18] J. Ambjorn, T. Askgaard, H. Porter, and M. E. Shaposhnikov, Nucl. Phys. **B353**, 346 (1991).
[19] A. Rajantie, P. M. Saffin, and E. J. Copeland, Phys. Rev. D **63**, 123512 (2001).
[20] A. Tranberg and J. Smit, J. High Energy Phys. 11 (2003) 016.
[21] M. van der Meulen, D. Sexty, J. Smit, and A. Tranberg, J. High Energy Phys. 02 (2006) 029.
[22] E. Farhi, N. Graham, V. Khemani, R. Markov, and R. Rosales, Phys. Rev. D **72**, 101701(R) (2005). See also, M. van der Meulen, D. Sexty, J. Smit, and A. Tranberg, J. High Energy Phys. 02 (2006) 029.
[23] M. Gleiser and J. Thorarinson, Phys. Rev. D **76**, 041701 (R) (2007).
[24] M. Gleiser and J. Thorarinson, Phys. Rev. D **79**, 025016 (2009).
[25] M. Gleiser, B. Rogers, and J. Thorarinson, Phys. Rev. D **77**, 023513 (2008); M. Gleiser and R. Howell, Phys. Rev. Lett. **94**, 151601 (2005).
[26] M. Gleiser, Int. J. Mod. Phys. D **16**, 219 (2007).
[27] M. Gleiser and R. Howell, Phys. Rev. E **68**, 065203(R) (2003).
[28] M. Gleiser and A. F. Heckler, Phys. Rev. Lett. **76**, 180 (1996).
[29] Mustafa A. Amin, arXiv:1006.3075v1.